Article

Cell Reports

Telomere Recognition and Assembly Mechanism of Mammalian Shelterin

Graphical Abstract

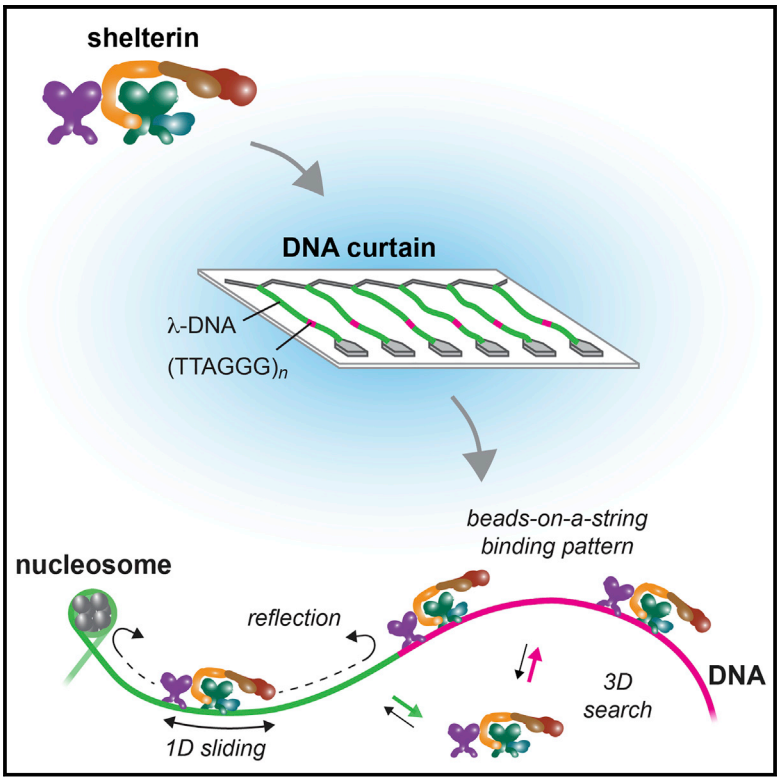

Authors

Fabian Erdel, Katja Kratz, Smaranda Willcox, Jack D. Griffith, Eric C. Greene, Titia de Lange

Correspondence

ecg2108@cumc.columbia.edu (E.C.G.), delange@rockefeller.edu (T.d.L.)

In Brief

The shelterin complex safeguards mammalian telomeres. Erdel et al. purify the full shelterin complex and visualize how individual complexes interact with DNA. They find that preassembled shelterin complexes can exist in solution and can rapidly find telomeric repeats by three-dimensional diffusion to ensure efficient and persistent telomere protection.

Highlights

- Shelterin can exist as a complex in solution
- Shelterin can diffuse along DNA but is impeded by nucleosomes
- Shelterin rapidly locates telomeric repeats by a three-dimensional diffusive search
- Shelterin forms ternary complexes with single- and double-stranded telomeric DNA

Erdel et al., 2017, Cell Reports *18*, 41–53
January 3, 2017
http://dx.doi.org/10.1016/j.celrep.2016.12.005

CellPress

Cell Reports
Article

Telomere Recognition and Assembly Mechanism of Mammalian Shelterin

Fabian Erdel,[1,4] Katja Kratz,[2,4] Smaranda Willcox,[3] Jack D. Griffith,[3] Eric C. Greene,[1,*] and Titia de Lange[2,5,*]
[1]Department of Biochemistry and Molecular Biophysics, Columbia University, New York, NY 10032, USA
[2]Laboratory for Cell Biology and Genetics, Rockefeller University, New York, NY 10065, USA
[3]Lineberger Comprehensive Cancer Center, University of North Carolina at Chapel Hill, Chapel Hill, NC 27599, USA
[4]Co-first author
[5]Lead Contact
*Correspondence: ecg2108@cumc.columbia.edu (E.C.G.), delange@rockefeller.edu (T.d.L.)
http://dx.doi.org/10.1016/j.celrep.2016.12.005

SUMMARY

Shelterin is a six-subunit protein complex that plays crucial roles in telomere length regulation, protection, and maintenance. Although several shelterin subunits have been studied in vitro, the biochemical properties of the fully assembled shelterin complex are not well defined. Here, we characterize shelterin using ensemble biochemical methods, electron microscopy, and single-molecule imaging to determine how shelterin recognizes and assembles onto telomeric repeats. We show that shelterin complexes can exist in solution and primarily locate telomeric DNA through a three-dimensional diffusive search. Shelterin can diffuse along non-telomeric DNA but is impeded by nucleosomes, arguing against extensive one-dimensional diffusion as a viable assembly mechanism. Our work supports a model in which individual shelterin complexes rapidly bind to telomeric repeats as independent functional units, which do not alter the DNA-binding mode of neighboring complexes but, rather, occupy telomeric DNA in a "beads on a string" configuration.

INTRODUCTION

Telomeres mark the ends of linear chromosomes and are important for maintaining genomic integrity. Mammalian telomeres contain the six-subunit protein complex shelterin (de Lange, 2005), which prevents recognition of chromosome ends as DNA breaks, in part by forming the t-loop structure (Doksani et al., 2013; Griffith et al., 1999). The protective function of shelterin prevents activation of DNA damage signaling pathways at chromosome ends and blocks double-strand break (DSB) repair pathways, which could lead to chromosome end fusions and other detrimental outcomes (Denchi and de Lange, 2007; Palm and de Lange, 2008; Sfeir and de Lange, 2012). The homodimeric TRF1 and TRF2 subunits in shelterin bind to telomeric double-stranded DNA (dsDNA), whereas the POT1 subunit binds telomeric single-stranded DNA (ssDNA). The TIN2 and TPP1 subunits connect the three DNA-binding proteins, and the sixth subunit, Rap1, is associated with TRF2.

Although the entire shelterin complex consists of TRF1, TRF2, Rap1, TIN2, TPP1, and POT1, sub-complexes lacking TRF1 or TRF2/Rap1 can engage telomeres in vivo (Celli and de Lange, 2005; Sfeir et al., 2009). Interaction of POT1 with telomeric ssDNA is not required for the telomeric localization of the rest of shelterin (Hockemeyer et al., 2006). Moreover, the interaction of POT1 with telomeric ssDNA is neither required nor sufficient for its localization to telomeres (Loayza and De Lange, 2003). Instead, POT1 is recruited to telomeres based on its interaction with TPP1 (Hockemeyer et al., 2007; Kibe et al., 2010; Liu et al., 2004; Ye et al., 2004).

Several shelterin subunits and some of the heterodimers in shelterin (e.g., POT1/TPP1, TRF2/Rap1) have been studied in vitro. This body of work has defined the DNA-binding activity of TRF1, TRF2, and POT1 and has elucidated the protein interactions among shelterin components (Palm and de Lange, 2008). TRF1 and TRF2 both contain C-terminal SANT/Myb DNA-binding domains that confer specificity for the highly conserved telomeric sequence 5′-YTAGGGTTR-3′ in dsDNA (Bianchi et al., 1999; Court et al., 2005; Hanaoka et al., 2005). TRF1 and TRF2 homodimerize, which is a requirement for their binding to telomeric repeats (Bianchi et al., 1997, 1999; Broccoli et al., 1997; van Steensel and de Lange, 1997; van Steensel et al., 1998). While TRF1 is mainly involved in telomeric DNA replication (Martínez et al., 2009; Sfeir et al., 2009), TRF2 is implicated in the formation of t-loops and suppression of ATM activation (Celli and de Lange, 2005; Denchi and de Lange, 2007; Doksani et al., 2013; Griffith et al., 1999; Karlseder et al., 1999, 2004). TRF2 has been shown to induce higher-order structures in DNA in vitro, including t-loops (Benarroch-Popivker et al., 2016; Gaullier et al., 2016; Griffith et al., 1999; Kaur et al., 2016; Stansel et al., 2001). A recent single molecule study has shown that isolated TRF1 and TRF2 can diffuse along DNA to locate telomeric repeats (Lin et al., 2014).

POT1 has two OB (oligonucleotide- or oligosaccharide-binding) folds in its N terminus that recognize the sequence 5′-TAGGGTTAG-3′ in telomeric ssDNA (Baumann and Cech, 2001; Lei et al., 2004; Loayza et al., 2004). TPP1 enhances the interaction of POT1 with telomeric DNA although TPP1 does not make contacts with the DNA substrate (Nandakumar and Cech, 2012; Taylor et al., 2011; Wang et al., 2007; Xin et al.,

2007). Mouse shelterin has two POT1 proteins, POT1a and POT1b, which have the same DNA-binding properties (Palm et al., 2009) but serve different tasks with POT1a being responsible for suppression of ATR activation and POT1b functioning in 3′ overhang regulation (Hockemeyer et al., 2006; Wu et al., 2006, 2012).

Despite the extensive characterization of the DNA-binding proteins in shelterin, information on the behavior of fully assembled shelterin complexes in vitro is currently lacking. In particular, it is unclear whether the shelterin complex is stable in solution or whether shelterin complexes can interact with each other to promote mutual stabilization and chromatin compaction as was recently proposed (Bandaria et al., 2016). It is also not known how shelterin assembles onto telomeric repeat sequences within the genome.

To address these questions, we combined ensemble biochemistry, electron microscopy, and single-molecule imaging with DNA curtains to study the DNA-binding features of purified shelterin. We found that shelterin could exist as an intact complex in solution and could diffuse in one dimension (1D) along DNA. However, this type of diffusion was impaired by DNA-bound obstacles like nucleosomes or other shelterin complexes, and 1D diffusion was not required for efficient recognition of telomeric repeat sequences. Rather, our results show that shelterin can rapidly locate telomeric repeats using a three-dimensional (3D) diffusive search. Shelterin in complex with telomeric ssDNA readily bound telomeric dsDNA, suggesting that t-loop formation can proceed via simultaneous capture of double-stranded telomeric repeats and the telomeric 3′ overhang by shelterin. The interaction among shelterin complexes bound to the same or different DNA molecule(s) was too weak to promote formation of extended filaments or to efficiently associate different DNA molecules, suggesting that shelterin recruitment and stabilization does not involve strong protein-protein interactions between shelterin complexes. Our findings suggest a model in which telomeres are composed of independently acting shelterin complexes bound to arrays of TTAGGG repeats rather than continuous shelterin filaments.

RESULTS

Characterization of Purified Shelterin

To study the biochemical properties of shelterin, we purified TRF2 alone, TRF2/Rap1, shelterin (TRF1/TRF2/Rap1/TIN2/TPP1/POT1a), and a shelterin complex lacking POT1a (Figure 1A) from co-transfected HEK293T cells. TRF2/Rap1, shelterin, and shelterin without POT1a were purified by a two-step isolation using N-terminal StrepII tags on TRF2, Rap1 or TPP1, and an N-terminal His tag on TRF2 (for TRF2/Rap1) or TRF1 (for shelterin ± POT1a). TRF2 (without Rap1) was isolated in a single step using the StrepII tag (Supplemental Experimental Procedures). A Coomassie gel indicated that each protein preparation was >90% pure although the shelterin preparations contained two contaminants that migrated close to POT1a (Figure 1B). Individual bands in the Coomassie gel were assigned to shelterin components by purifying and analyzing complexes with different combinations of subunits (Figure S1A). In addition, the identity of each band was confirmed by mass spectrometry (Figures S1A and S1B). BSA standards were used to approximate the TRF2 protein concentration in each preparation, and all experiments were performed with the concentration of the complexes normalized based on their TRF2 content (Figures 1B and 1C). The presence of the respective subunits in each preparation was verified by immunoblotting (Figure 1C), and the absence of human shelterin components that might have copurified with the mouse shelterin complex was confirmed (Figures S1C and S1D). Each shelterin subunit showed the expected molecular weight with the exception of Rap1, which migrated differently depending on the tag (StrepII or Flag) at its N terminus (Figures 1A–1C). The stoichiometry of TRF2/Rap1 was close to 1:1 as expected based on previous work (Zhu et al., 2000). The stoichiometry of the isolated shelterin complexes suggested a slight excess of TPP1, TIN2, and TRF1, as is expected from the purification strategy. Because the TPP1 and TIN2 subunits in shelterin are often phosphorylated in HEK293T cells, the preparations were treated with phosphatase before gel analysis. However, all other experiments were carried out without phosphatase treatment.

The isolated proteins were subjected to electrophoretic mobility shift assay (EMSA) DNA-binding studies with a 195-bp DNA fragment containing 32 telomeric repeats. All complexes showed robust binding to this substrate. To verify the presence of the various shelterin subunits in the complexes, antibody supershift experiments were performed (Figure 1D). As controls for these experiments, an unrelated antibody (to α-tubulin) was used. Furthermore, we confirmed that none of the antibodies bound to naked DNA. As expected, the antibody to TRF2 resulted in a supershift of the TRF2-DNA complex and the α-Rap1 antibody induced a supershift of the TRF2/Rap1 complex bound to DNA. Antibodies against Rap1, TRF1, and the StrepII tag (for StrepII-Myc-TPP1) confirmed the presence of these shelterin subunits in the DNA-bound shelterin complexes. Although the supershift with the α-TRF1 and α-StrepII antibodies was less pronounced than with other antibodies, side-by-side comparison showed a reproducible retardation of the shelterin-DNA complex, indicating that TRF1 and TPP1 were present. TIN2 was inferred to be present based on the presence of TPP1, which requires TIN2 for its association with TRF1 and TRF2. The presence of POT1a in the DNA-bound shelterin complex was verified as described below.

Binding of Shelterin to Telomeric Substrates Is Improved by POT1a

Specific binding to telomeric DNA was confirmed by EMSAs of TRF2, TRF2/Rap1, and shelterin with and without POT1a in the presence of either telomeric or non-telomeric dsDNA (Figures 2A–2D). Each preparation bound to the telomeric dsDNA and showed little interaction with non-telomeric dsDNA in three independent experiments using two different protein preparations. To compare the relative binding strength of the different complexes, we determined the apparent dissociation constant (K_D) for binding of TRF2, TRF2/Rap1, and shelterin with and without POT1a to a 195-bp substrate of telomeric dsDNA based on the disappearance of the unbound DNA (see Supplemental Experimental Procedures for fit function). TRF2, TRF2/Rap1, and the shelterin complexes showed the same apparent K_D of ~1 nM for the 195-bp telomeric dsDNA substrate. Therefore, the

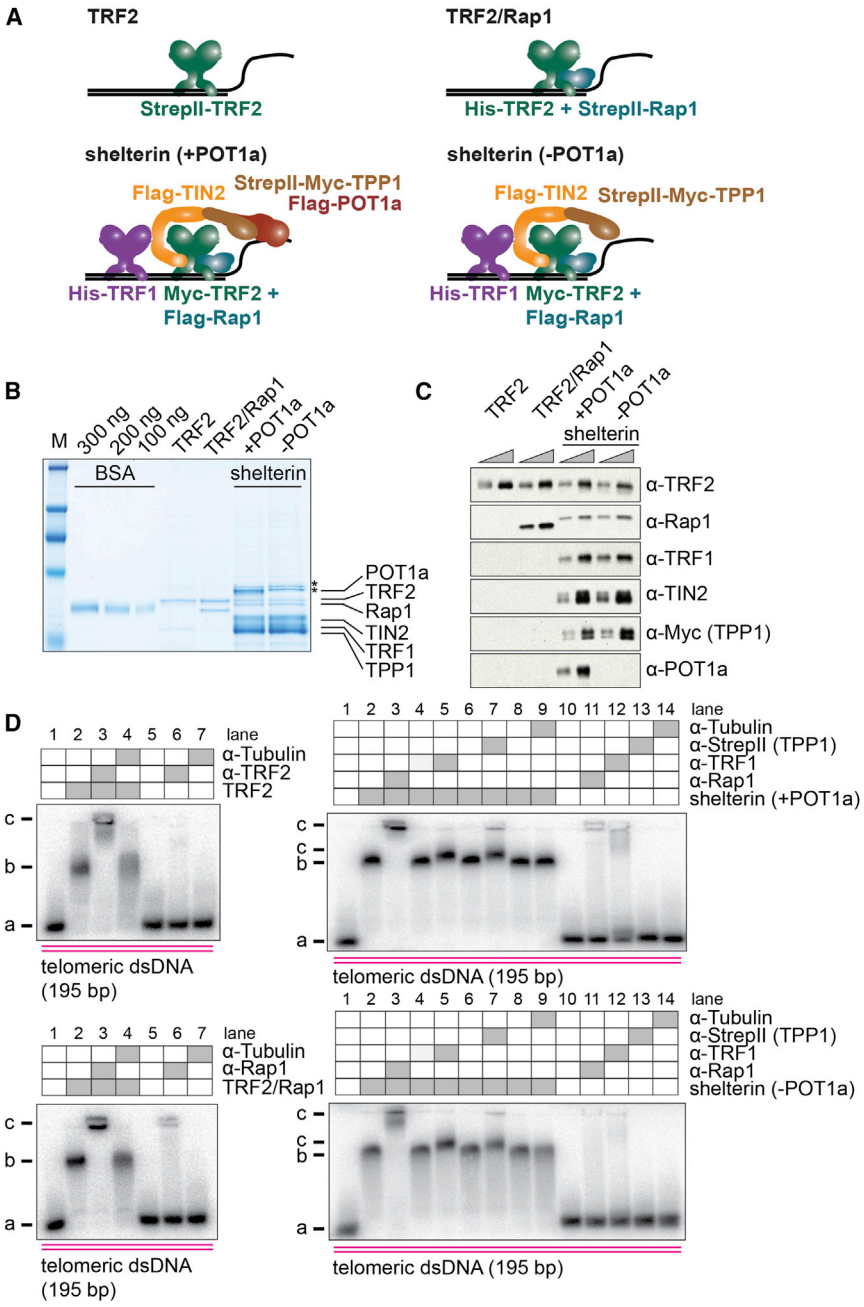

Figure 1. Purification and Biochemical Characterization of Shelterin Complexes

(A) Overview of TRF2, TRF2/Rap1, shelterin (+POT1a), and shelterin (–POT1a) used in this study.

(B) Coomassie-stained SDS gel showing an example of purified TRF2, TRF2/Rap1, shelterin (+POT1a), and shelterin (-POT1a). *Contaminant. See also Figure S1.

(C) Immunoblot for shelterin subunits of purified TRF2, TRF2/Rap1, shelterin (+POT1a), and shelterin (–POT1a). Protein amounts were adjusted using TRF2 as a reference. See also Figure S1.

(D) EMSA supershifts showing the stability of isolated TRF2, TRF2/Rap1, shelterin (+POT1a), and shelterin (–POT1a) complexes when bound to telomeric dsDNA. a, free DNA; b, protein-DNA complexes; c, supershifts.

presence of both TRF1 and TRF2 in shelterin did not substantially increase the binding to telomeric dsDNA under these conditions. In contrast, in vivo data suggest that the accumulation of shelterin at telomeres is improved by the presence of both TRF1 and TRF2 and their TIN2 link (Celli and de Lange, 2005; Sfeir et al., 2009; Takai et al., 2011).

The interaction of POT1a with telomeric ssDNA substantially altered the apparent K_D of shelterin for telomeric substrates. A short telomeric dsDNA substrate was generated that carried a single-stranded 3′ overhang of 36 nt with either non-telomeric or telomeric sequence (Figures 2E and 2F). In three independent experiments using two different protein preparations, binding of shelterin to the substrate with a non-telomeric overhang was not significantly affected by the presence of POT1a in the complex (apparent K_D of 1.1 and 2.3 nM with and without POT1a, respectively) (Figure 2E). However, when the substrate carried POT1a-binding sites in the 3′ overhang, the apparent dissociation constant of shelterin containing POT1a was ~0.1 nM, which is 16 times lower than the K_D for this substrate when shelterin lacked POT1a (Figure 2F). This improved affinity afforded by the engagement of POT1a with its ssDNA recognition sequence is consistent with a previous report (Choi et al., 2011) and provides evidence for the presence of POT1a in the purified shelterin complex.

TRF2/Rap1 and Shelterin Show a Similar Preference for Telomeric dsDNA

To visualize the interaction of individual shelterin complexes with DNA, we used single-tethered DNA curtains (Greene et al., 2010), which were composed of hundreds of λ-DNA molecules containing an insert of 32 telomeric repeats (Figures 3A and S2). The telomeric insert corresponded to the substrate used for the EMSAs in Figures 2A–2D. Curtains were assembled on nanofabricated glass slides with a chrome barrier that served for alignment of individual DNA molecules. In the presence of buffer flow, DNA molecules and bound proteins were extended and brought close to the glass surface, where they could be visualized using total internal reflection fluorescence (TIRF) microscopy. In the absence of buffer flow, the bulk of the DNA molecules diffused away from the surface and consequently left the field of view although

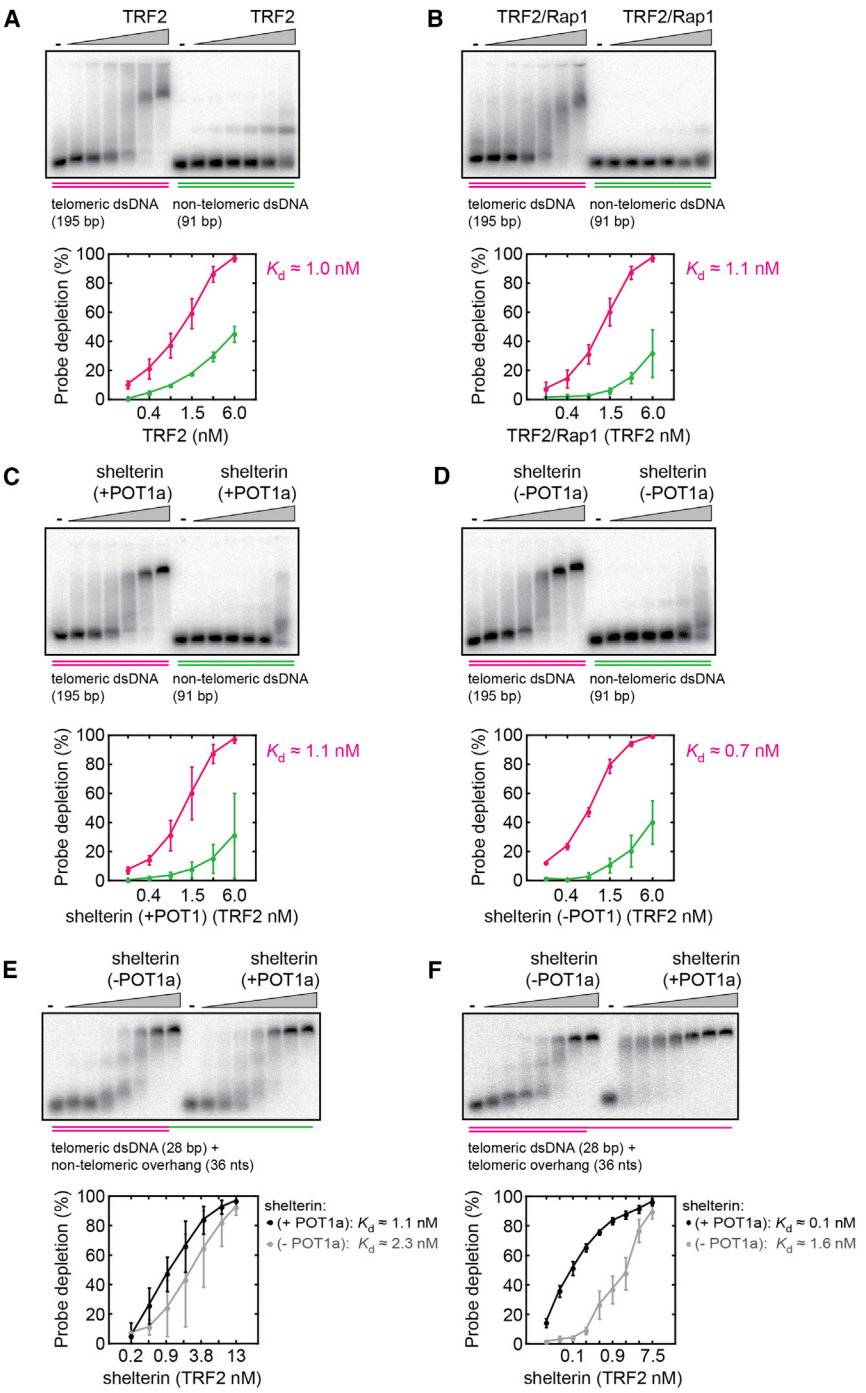

Figure 2. DNA-Binding Properties of TRF2, TRF2/Rap1, and Shelterin with and without POT1a

(A–D) EMSAs showing the telomeric dsDNA-binding specificity of TRF2 (A), TRF2/Rap1 (B), shelterin (+POT1a) (C), and shelterin (-POT1a) (D) when titrated on both telomeric and non-telomeric dsDNA. Apparent dissociation constants refer to the binding interaction with a 195-bp telomeric substrate. Data are represented as mean ± SD of three independent experiments using two different protein purifications.

(E and F) Shelterin (–POT1a) and shelterin (+POT1a) complexes were titrated on telomeric dsDNA that contained either a single-stranded non-telomeric (E) or single-stranded telomeric (F) overhang. Apparent dissociation constants refer to the binding interaction with a 28-bp substrate with a telomeric or non-telomeric 3′ overhang. Data are represented as mean ± SD of three independent experiments using two different protein purifications.

one end of the DNA molecules remained tethered to the surface (Figure 3A). Therefore, DNA-bound proteins could be distinguished from proteins that might have been non-specifically bound to the surface based on their different behavior in the presence or absence of flow.

To visualize TRF2/Rap1, the N-terminal SNAP tag of Rap1 was conjugated with an Alexa Fluor 647 dye. Labeled complexes were incubated with a DNA curtain, and unbound proteins were removed by buffer flow. TIRF images show that TRF2/Rap1 preferentially bound the λ-DNAs at the site corresponding to the position of the telomeric DNA insert approximately 15 kb from the free DNA end (Figure 3B). To validate that the binding distribution of TRF2/Rap1 was determined by the telomeric sequence, we incubated TRF2/Rap1 with a different DNA substrate, in which the telomeric insert was moved to another position within the λ-DNA (scheme in Figure S2A). As expected, TRF2/Rap1 was again enriched at the telomeric insert (Figure S3A), which for this substrate was located near the center of the DNA molecule approximately 24 kb from the DNA ends.

To visualize shelterin, the complex (composed of TRF1, TRF2, Rap1, TIN2, TPP1, and POT1a) was labeled via conjugation of the Alexa Fluor 647 dye to the N-terminal SNAP tag of POT1a. Because POT1a does not bind to dsDNA, this strategy ensured that labeled complexes that resided on DNA curtains contained TRF1 and/or TRF2, which are required for dsDNA binding, and TIN2 and TPP1, which are required for the association of POT1a with TRF1 or TRF2. Similar to TRF2/Rap1, shelterin showed preferential binding to the telomeric insert (Figure 3C). Buffer flow was switched on and off to validate that labeled complexes were associated with DNA molecules (Figure 3C; Movie S1). Similar to the full complex, shelterin complexes lacking POT1a, which were labeled via conjugation of Alexa Fluor 647 to the N-terminal SNAP tag of Rap1, also bound preferentially to the DNA region containing telomeric repeats (Figure S3B).

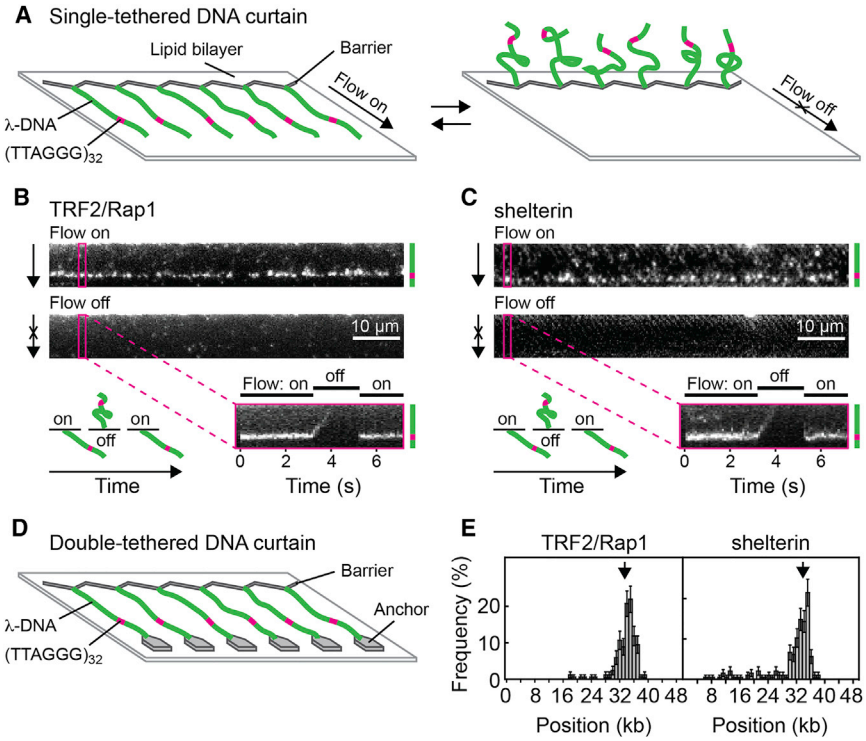

Figure 3. Individual Shelterin Complexes Display a Strong Preference for Telomeric Repeats

(A) Schematic of a single-tethered DNA curtain with and without buffer flow. Curtains were made of λ-DNA containing an insert of 32 telomeric repeats (magenta). See also Figure S2.

(B) Individual TRF2/Rap1 complexes labeled via SNAP647-Rap1 exhibited a strong preference for telomeric repeats. To validate that labeled proteins were bound to DNA, the fluorescence signal was recorded in the presence and absence of flow.

(C) Shelterin complexes labeled via SNAP647-POT1a displayed a similar preference for telomeric repeats as TRF2/Rap1 in Figure 3B. See also Movie S1.

(D) Double-tethered DNA curtains were composed of DNA molecules that were anchored to the surface on both ends.

(E) Histogram of the positions of TRF2/Rap1 and shelterin complexes bound to double-tethered DNA molecules. Arrows indicate the position of the telomeric insert. Error bars were determined based on bootstrapping (Experimental Procedures). See also Figure S3.

Thus, consistent with the EMSA data presented in Figure 2, the DNA-binding specificity of TRF2/Rap1 and shelterin appear similar and result in robust recognition of telomeric repeats in the context of an ~250 times excess of non-telomeric λ-DNA.

Next, we used double-tethered DNA curtains to determine the binding position of TRF2/Rap1 and shelterin. Double-tethered curtains contained an additional chrome anchor so that DNA molecules were tethered to the surface at both ends (Figure 3D). Accordingly, DNA molecules remained extended in the absence of buffer flow and binding positions could be mapped in the absence of flow-induced hydrodynamic force. The histograms for the localization of TRF2/Rap1 and shelterin along the DNA molecules (Figure 3E) indicated that both complexes showed a strong preference for telomeric repeats (black arrows).

Telomere Recognition Mechanism of TRF2/Rap1

To determine how TRF2/Rap1 recognizes telomeric repeats, we followed its target search process in real-time (Movie S2). To this end, we pre-labeled TRF2/Rap1 with a primary antibody against Rap1 and a quantum dot (QDot)-coupled secondary antibody before the complex was added to the DNA curtain (Figure 4A, top). As QDots are photo-stable, this approach allowed for prolonged imaging of TRF2/Rap1 at high temporal resolution.

After injection of TRF2/Rap1 complexes onto the DNA curtain, we switched the buffer flow off and recorded the initial binding position for each complex that associated with a double-tethered DNA molecule (Figure 4A, bottom). The histogram of initial binding positions exhibited a peak at the telomeric insert, suggesting that a considerable fraction of complexes (~57% of stable binders) directly recognized telomeric repeats by 3D diffusion in the surrounding buffer without extensively diffusing along the flanking DNA. Furthermore, we determined the lifetime for each DNA-bound complex (Figure 4B; Table S1). Lifetimes were considerably shorter at non-telomeric DNA ($t_{1/2}$ ≈6–38 s) than at telomeric repeats ($t_{1/2}$ >23 min). The lifetime at telomeric repeats represents a lower limit because on this time-scale double-tethered DNA molecules start dissociating from their anchors, which leads to apparent dissociation events even though the proteins stay associated with their binding sites. A small population of binding events with short lifetimes ($t_{1/2}$ ≈100 s) was also observed at the region of DNA containing the telomeric insert. These events probably represent binding interactions with non-telomeric DNA adjacent to the telomeric repeats that at our spatial resolution cannot be distinguished from the telomeric insert.

Although TRF2/Rap1 complexes showed a preference for directly recognizing telomeric repeats by 3D diffusion (Figure 4C, upper panel), a subpopulation (~43% of stable binders) of TRF2/Rap1 complexes bound to non-telomeric DNA first and diffused in 1D along the DNA until the repeats were stably bound (Figure 4C, lower panel). A quantification of the different populations is shown in Figure 4D. To probe the influence of 1D diffusion on the target search process, we conducted real-time binding measurements at an elevated ionic strength of 300 mM potassium glutamate, which severely reduced the interaction of TRF2/Rap1 with non-telomeric DNA (Figure S4A). Under these conditions, TRF2/Rap1 readily bound to telomeric repeats (Figure S4B), corroborating the finding that 1D diffusion on extended stretches of non-telomeric DNA is not a prerequisite for efficient recognition of telomeric repeats.

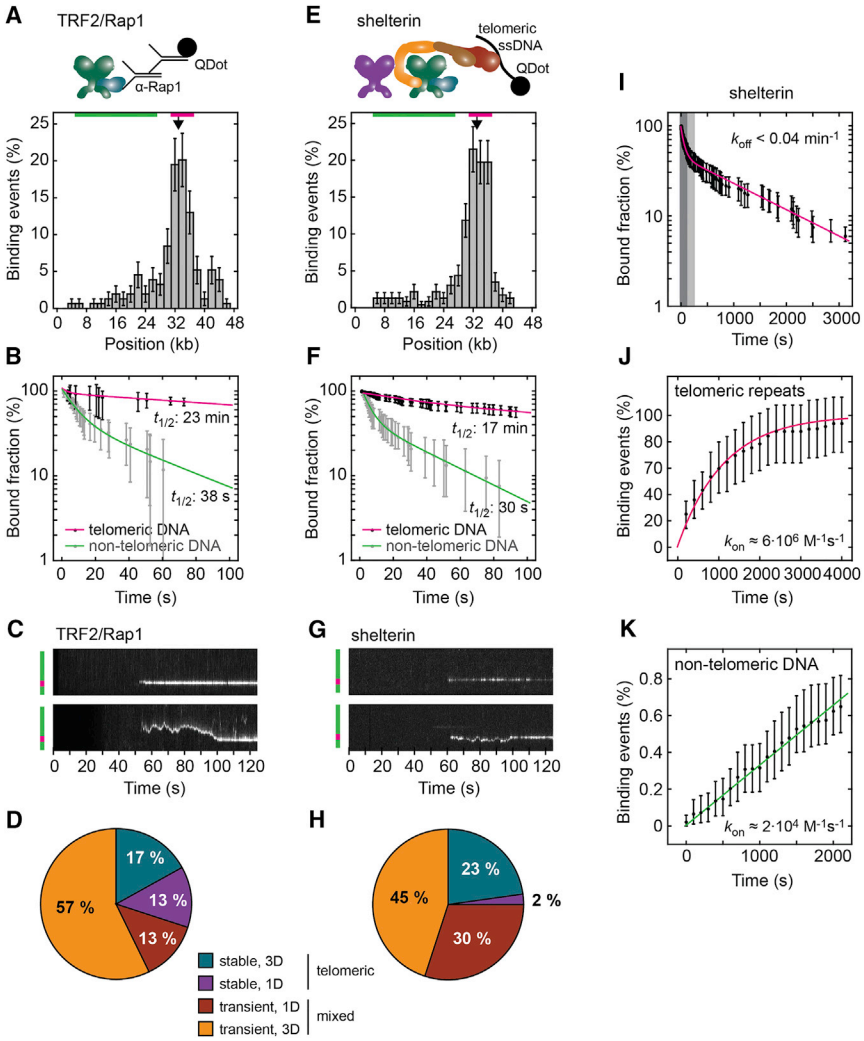

Figure 4. Binding Kinetics and Search Mechanism of Shelterin Complexes

(A) Histogram of the initial DNA-binding positions of QDot-labeled TRF2/Rap1 complexes. See also Figure S4.

(B) Survival probability plot showing the fraction of TRF2/Rap1 complexes that was still bound to the telomeric (black, magenta fit) and non-telomeric (gray, green fit) DNA after a given time. For fit results, see Table S1.

(C) Kymograms showing individual TRF2/Rap1 complexes that bound to the telomeric insert via 3D (top) or 1D (bottom) search mechanisms. See also Figure S5 and Movie S2.

(D) Overview of the interaction behavior of TRF2/Rap1 with DNA. Stable interactions were restricted to telomeric inserts, whereas transient interactions were observed across the entire DNA.

(E) Histogram of the initial DNA-binding positions of QDot-labeled shelterin complexes.

(F) Survival probability plot showing the fraction of shelterin complexes that was still bound to the telomeric (black, magenta fit) and non-telomeric (gray, green fit) DNA after a given time. For fit results, see Table S1.

(G) Kymograms showing individual shelterin complexes that bound to the telomeric insert via 3D (top) or 1D (bottom) search mechanisms. See also Figure S6.

(H) Overview of the interaction behavior of shelterin with DNA. Stable interactions were restricted to telomeric inserts, whereas transient interactions were observed across the entire DNA. For legend, see Figure 4D.

(I) Survival probability plot for molecules bound to the telomeric insert reveals two populations with very different lifetimes. The stably bound population exhibits mono-exponential decay kinetics with k_{off} = 0.04 min^{-1}. The events with lifetimes above 250 s (white region) were considered for the association rate measurement in Figure 4J, events with lifetimes below 120 s (dark gray region) were considered for the association rate measurement in Figure 4K.

(J and K) After injection of pre-labeled shelterin complexes, the number of long-lived (J) and short-lived (K) binding events was followed over time. The on rates were determined as described in Supplemental Experimental Procedures.

Error bars in this figure were determined based on bootstrapping.

To test whether TRF2/Rap1 behaved differently from TRF2 in isolation, we conducted similar experiments with TRF2 that was pre-labeled with an antibody against TRF2 and a QDot-coupled secondary antibody (Figures S5A–S5C). Like TRF2/Rap1, TRF2 alone preferentially associated with telomeric repeats (see Figure S5A for a representative kymogram). Furthermore, TRF2 could stably bind to telomeric repeats for several minutes without dissociating or diffusing onto the adjacent non-telomeric DNA (see Figure S5B for a representative kymogram). These experiments suggest that TRF2 and TRF2/Rap1 interact similarly with dsDNA.

Telomere Recognition Mechanism of Shelterin

We next determined how shelterin searches for telomeric repeats. Shelterin was pre-labeled with a fluorescent single-stranded telomeric oligonucleotide that binds to POT1a (Figure 4E, top). Complexes with POT1a-bound ssDNA mimic the presumed state of shelterin bound to both dsDNA and ssDNA as it would occur at the telomere terminus or close to the D loop of the t-loop structure. The binding process of these complexes was monitored as described above for TRF2/Rap1. Similar to TRF2/Rap1, shelterin preferentially associated with telomeric repeats (Figure 4E, bottom), forming ternary complexes that simultaneously contacted telomeric dsDNA and ssDNA. These complexes were much more stable at telomeric repeats ($t_{1/2} \geq 17$ min) than on non-telomeric dsDNA ($t_{1/2} \approx 4$–30 s) (Figure 4F; Table S1). As discussed for TRF2/Rap1 above the lifetime observed at telomeric repeats represents a lower limit because signal loss might also have been due to dissociation of double-tethered DNA molecules from their anchors. Like TRF2/Rap1, shelterin complexes could locate telomeric repeats by either 1D or 3D diffusion (Figure 4G). Quantification of the different populations (Figure 4H) showed that, in contrast to TRF2/Rap1, only 2% of shelterin complexes (8% of stable binders) located

telomeric repeats using 1D diffusion across an extended portion of non-telomeric DNA (see Figure 4G for an example).

To assess the integrity of the shelterin complexes observed here, we simultaneously labeled Rap1 (according to the scheme in Figure 4A, top) and POT1a (according to the scheme in Figure 4E, top) with QDots of different colors and repeated the experiment above. Roughly half of the observed complexes that bound to the DNA curtain contained labeled telomeric ssDNA, and ~96% of this population also contained labeled Rap1 (Figure S6A). Due to the simultaneous presence of POT1a and Rap1 these double-labeled complexes must also contain TIN2, TPP1, and TRF2, which are required for the association of POT1a with Rap1. A representative kymogram showing a double-labeled shelterin complex that binds to the telomeric dsDNA insert is shown in Figure S6B. These observations suggest that intact shelterin complexes can exist in solution and bind to DNA as one entity. The fact that only half of the complexes contained labeled telomeric ssDNA might be due to incomplete labeling or due to a subpopulation of complexes that lacked POT1a.

Finally, we sought to determine the association rate for shelterin binding to telomeric repeats. To this end, we focused on binding events with a lifetime of at least 250 s, which represent the stably bound fraction (Figure 4I). These long-lived events were exclusively observed at the telomeric insert. We summed the number of these binding events over time (Figure 4J) and fitted the resulting curve as described in the Supplemental Experimental Procedures, yielding an on rate of $\sim 6 \times 10^6$ $M^{-1}s^{-1}$ (Figure 4J; Table S1). The association rate for short-lived interactions with lifetimes below 120 s, derived in a similar manner, yielded an on rate of $\sim 2 \times 10^4$ $M^{-1}s^{-1}$ (Figure 4K; Table S1). Short-lived binding events were observed across the entire λ-Telo DNA molecule and therefore represent shelterin interactions with non-telomeric DNA. The curve for these short-lived events (Figure 4K) has a different shape than that for telomeric binding events (Figure 4J) because the experiments were conducted at a shelterin concentration at which telomeric binding sites reached saturation over time, whereas non-telomeric binding sites never reached saturation due to their lower affinity. Both on rates refer to 195-bp stretches of telomeric or non-telomeric DNA. TRF2/Rap1 behaved similarly to shelterin, with an on rate of $\sim 2 \times 10^6$ $M^{-1}s^{-1}$ at telomeric repeats (Figure S6C) and an on rate of $\sim 3 \times 10^4$ $M^{-1}s^{-1}$ at non-telomeric DNA (Figure S6D).

These results indicate that TRF2/Rap1 and shelterin share a common telomere recognition mechanism; i.e., they primarily recognize telomeric repeats by a 3D search. The on rate measurements suggest that, upon sampling the DNA, the probability to transition into a DNA-bound state that is stable enough to be resolved in our experiments is ~100 times larger at the telomeric insert than at a non-telomeric DNA stretch of identical size for both TRF2/Rap1 and shelterin.

Differential Interaction of Shelterin with Telomeric and Non-telomeric DNA

To further characterize the binding interactions of shelterin with telomeric and non-telomeric DNA, we used double-tethered DNA curtains composed of λ-DNA with or without a telomeric insert. We incubated shelterin with these double-tethered DNA curtains, removed unbound proteins by buffer flow and subsequently labeled the DNA-bound complexes with QDot-coupled antibodies. Individual shelterin complexes bound to and rapidly diffused along non-telomeric DNA (Movie S3) with the diffusion coefficients shown in Figure 5A. For the experiments with λ-DNA that contained a telomeric insert (λ-Telo), only positions without telomeric repeats were considered. An example of an individual shelterin complex that diffused across the entire length of a wild-type λ-DNA molecule is shown in Figure 5B (upper kymogram). The distribution of diffusion coefficients obtained in these experiments is shown in Figure 5C.

Shelterin interacts much stronger with telomeric repeats than with non-telomeric DNA (Figures 4F and 4I). Most shelterin complexes that were bound to telomeric repeats remained bound for tens of minutes without dissociating from the DNA or diffusing to the adjacent non-telomeric DNA portion. Shelterin complexes that moved along the non-telomeric DNA by 1D diffusion often encountered the stably bound shelterin complexes at telomeric repeats. In these cases, diffusing shelterin complexes were deflected from stably bound shelterin at the telomeric insert (lower panel in Figure 5B), indicating that shelterin complexes interacting with the same DNA molecule cannot bypass one another. Furthermore, when two shelterin complexes encountered one another they did not exhibit evidence of stable interactions with each other while bound to the same DNA. Similarly, shelterin complexes were deflected at nucleosomes that resided on non-telomeric DNA (Figure 5D).

In contrast to shelterin that was bound to telomeric repeats, shelterin bound to non-telomeric DNA could be pushed along the DNA by the hydrodynamic force imposed by buffer flow (Figure 5E), further demonstrating that the interaction of shelterin with non-telomeric sequences is much weaker than the interaction with telomeric repeats.

TRF2/Rap1 and Shelterin Behave as Independent DNA-Binding Entities

As shelterin occupies many kilobases of highly repetitive telomeric DNA in vivo, we probed the protein-protein interactions among DNA-bound shelterin complexes that might contribute to the stabilization of these structures and might cause telomere compaction. To address this question, we interrogated the *cis* interaction among complexes that were bound to telomeric and non-telomeric sequences on the same DNA molecule (Figure 5E). To test for *cis* interactions, we pushed shelterin associated with non-telomeric DNA along the DNA molecule by buffer flow until it contacted shelterin that was bound to the telomeric insert. Subsequently, we switched off buffer flow to monitor whether complexes that were pushed to the telomeric insert were retained there by protein-protein interactions (see representative kymograms in Figure 5E). Both shelterin and TRF2/Rap1 associated with non-telomeric DNA were readily pushed to the proteins on the telomeric insert. However, they began to diffuse along non-telomeric DNA within tens of seconds after flow had been turned off (Figures 5E and S7A), indicating that neither shelterin nor TRF2/Rap1 complexes on the same DNA molecule interacted with each other on this timescale. Note that the flow-induced reversible displacement of complexes bound to telomeric repeats reflects stretching and relaxation of

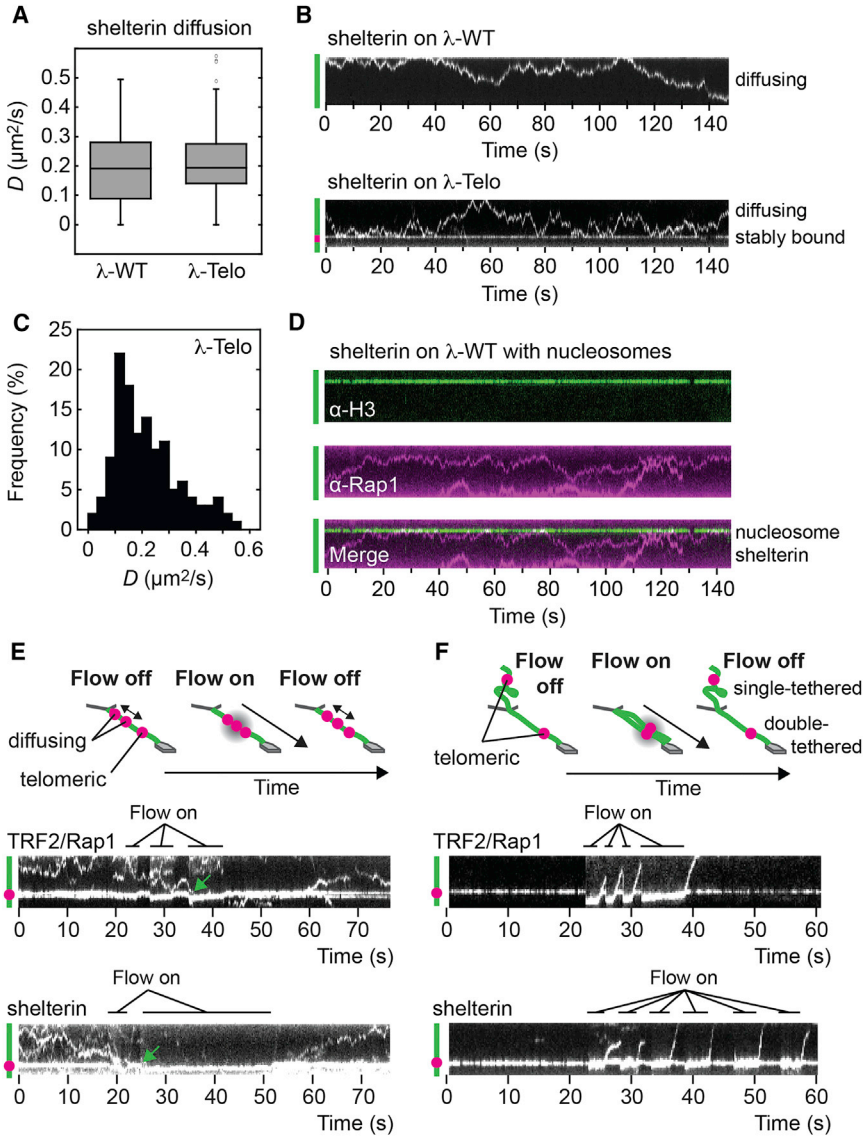

Figure 5. Shelterin Diffusion along Non-telomeric DNA

(A) Diffusion coefficients for individual shelterin complexes on non-telomeric DNA.

(B) Representative kymograms for diffusing shelterin on wild-type λ-DNA (top) and on λ-Telo DNA (bottom). See also Movie S3.

(C) Histogram of the diffusion coefficients obtained for shelterin on λ-DNA.

(D) Representative kymogram showing shelterin complexes (magenta) that diffused on non-telomeric DNA and were reflected at a nucleosome (green).

(E) Experimental strategy for testing TRF2/Rap1 or shelterin interactions in *cis* (top). Representative kymograms (bottom) show that the complexes did not stably interact with one another even when brought together by hydrodynamic force (green arrows), which we used to push shelterin complexes along non-telomeric DNA. For a quantitation, see Figure S7A.

(F) Experimental strategy for testing TRF2/Rap1 or shelterin interactions in *trans* (top). Representative kymograms show the absence of strong *trans* interactions between complexes bound to different DNA molecules. For a quantitation, see Figure S7B.

double-tethered DNA molecules. The observation that shelterin complexes on the same DNA molecule do not strongly interact with each other is consistent with the diffusion behavior of complexes that do not associate with each other after having collided (e.g., Figure 5B, lower kymogram).

To probe the *trans* interaction among shelterin complexes that were bound to telomeric repeats on different DNA molecules, we used a curtain composed of single- and double-tethered DNA molecules bound by shelterin or TRF2/Rap1 complexes at the telomeric inserts (Figure 5F). Complexes bound to different single- and double-tethered DNA molecules were brought into close spatial proximity using buffer flow, and interactions were probed by assessing the potential retention of single-tethered DNA molecules in the absence of buffer flow. As shown in the kymograms for shelterin and TRF2/Rap1, single- and double-tethered DNA molecules quickly separated as soon as the buffer flow was switched off. A quantitation is shown in Figure S7B. These observations argue against strong *trans* interactions among shelterin complexes bound to different DNA molecules, although we cannot exclude the presence of short-lived interactions or association reactions with a low on rate.

Shelterin Density and Binding Configuration at Telomeric Repeats

To further examine the propensity of shelterin to form filaments, we sought to quantify the number of labeled complexes bound to the telomeric insert after a 10-min incubation of 2 nM shelterin, which is in the range of the apparent dissociation constants found above (Figures 2A–2D) and similar to the free concentration of shelterin components in the nucleoplasm (Takai et al., 2010). To this end, we analyzed the intensity of complexes at telomeric inserts over time (Figures 6A–6D). As individual dye-labeled molecules bleach when illuminated by laser light, a stepwise decrease in intensity was observed (see Figures 6A and 6B for representative bleaching traces). We estimated the number of labeled proteins present at the insert by analyzing the initial signal intensity (Figure 6C) and by counting the number of photobleaching steps (Figure 6D), which yields a conservative estimate for the number of dye molecules because not every step can be clearly distinguished. Assuming the presence of two labeled Rap1 molecules in each TRF2/Rap1 complex, one to two complexes were present on the telomeric repeat array. Similarly, one to two shelterin units (each containing one labeled POT1a molecule) were associated with the telomeric repeat

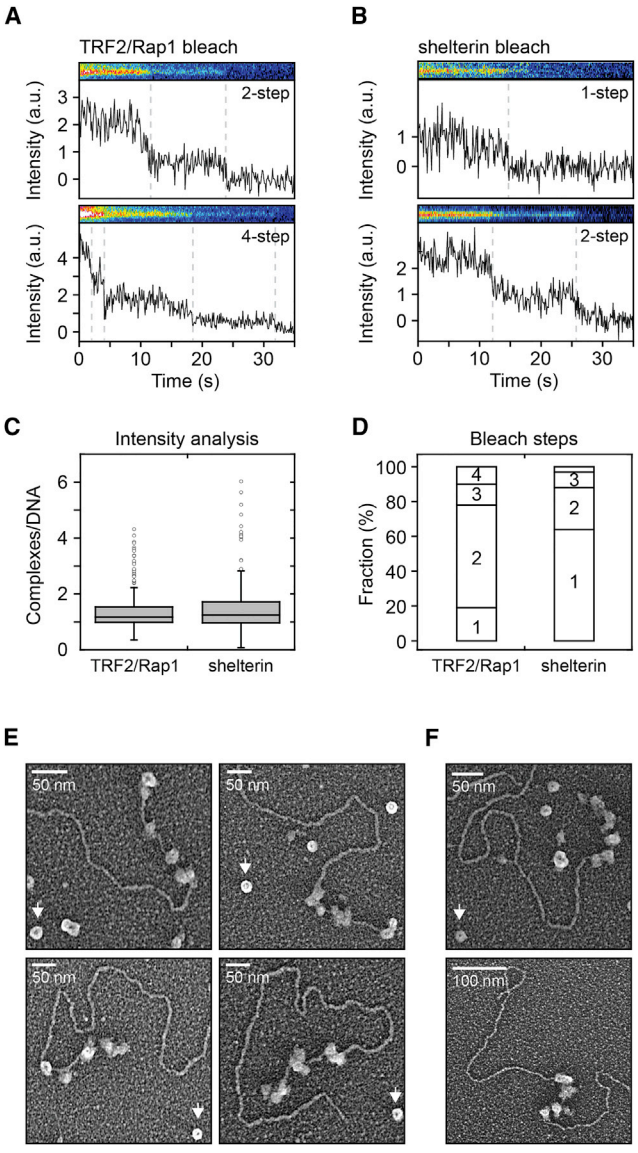

Figure 6. Shelterin Density at Telomeric Repeats

(A) Representative photobleaching traces for TRF2/Rap1 complexes at individual telomeric inserts. Kymograms are shown on top, the time evolution of the integrated intensity is plotted below.

(B) Representative photobleaching traces for shelterin complexes at individual telomeric inserts.

(C) Number of complexes bound to individual telomeric inserts determined based on their intensity before bleaching. The intensity at the telomeric insert was normalized relative to the intensity of complexes bound on non-telomeric DNA.

(D) Number of visible bleach steps for each type of complex.

(E) EM images showing individual shelterin complexes (+POT1a/b) bound to a terminally located stretch of 576 bp of telomeric repeats followed by a 54-nt single-stranded telomeric overhang under sub-saturating conditions. Ferritin (arrows) was added to the samples as size reference.

(F) EM images showing shelterin (+POT1a/b) bound to a terminally (top) or internally (bottom) located stretch of 576 bp of telomeric repeats under saturating conditions. Ferritin (arrows) was added to the samples as size reference.

array. These values represent lower limits because a fraction of DNA-bound proteins might be unlabeled. However, the result that each DNA molecule is associated with only one or a few shelterin complexes argues against a model in which initial binding of a shelterin complex on telomeric repeats would trigger rapid recruitment of additional shelterin complexes that would form an extended filament on the flanking DNA via protein-protein interactions.

Finally, we used electron microscopy (EM) to probe the interaction between unlabeled shelterin complexes and DNA. All shelterin complexes used for EM contained POT1a and POT1b, and the presence of all subunits was confirmed by immunoblotting. Except for TPP1, the shelterin subunits were untagged. Shelterin was incubated with linearized plasmids either containing 576 bp of 96 double-stranded telomeric repeats and a 54-nt telomeric overhang or containing the double-stranded telomeric repeats at an internal position. Most images showed a few shelterin complexes bound to the telomeric insert under sub-saturating conditions, regardless of its position within the linear DNA (Figures 6E and 6F). Ferritin (450 kDa) added to the samples showed that the bound shelterin complexes were of expected size because shelterin is predicted to be approximately 450 kDa. Importantly, most shelterin complexes that were bound to their substrate did not contact each other (Figure 6E), suggesting that shelterin did not preferentially associate with another shelterin bound to the telomeric DNA as it would be expected in the presence of strong protein-protein interactions among different complexes. In addition, the EM analysis of saturated substrates (Figure 6F) did not show evidence of shelterin-mediated higher-order structures that might lead to compaction of telomeric chromatin as recently proposed (Bandaria et al., 2016).

In summary, these experiments suggest that shelterin complexes bind independently to telomeric repeats and can reach a density of roughly one shelterin per 100 bp.

DISCUSSION

The principal findings presented here are summarized in a quantitative model (Figure 7). They have implications for understanding the assembly of telomeric nucleoprotein complexes, the dynamics of shelterin at telomeres, and the proposed role of shelterin in telomere compaction as discussed below.

Shelterin Interaction with DNA

Shelterin complexes can bind to both telomeric and non-telomeric DNA (Figure 7A). Strong binding interactions are observed at telomeric DNA, which are reflected by a fast association rate, a slow dissociation rate and substantial resistance to hydrodynamic force and high ionic strength. In contrast, the interaction with non-telomeric DNA is salt-sensitive and transient, allowing for rapid 1D diffusion between different sites at low ionic strength and in the absence of DNA-bound obstacles. Consistently, these differences are reflected by the different binding strength to telomeric and non-telomeric DNA observed in ensemble biochemical experiments.

The interaction of GFP-tagged TRF1, TRF2, and POT1 with telomeres has previously been studied in living cells (Mattern

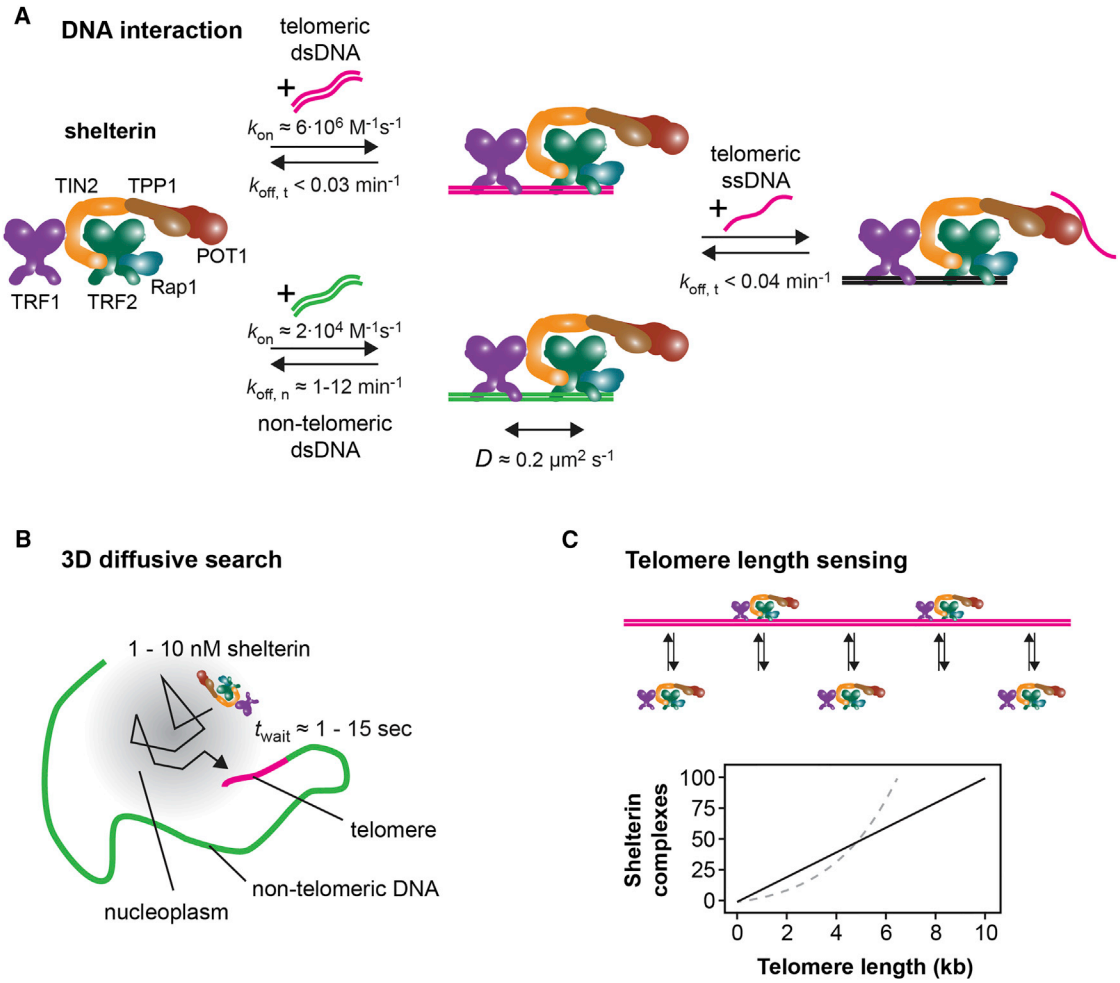

Figure 7. Interaction Behavior of Shelterin

(A) Shelterin can exist as a complex in solution and preferentially binds telomeric dsDNA. Shelterin can form stable ternary complexes that simultaneously bind telomeric ssDNA and dsDNA, e.g., at the telomere terminus that contains a 3′ overhang. Shelterin can diffuse along DNA unless it encounters obstacles like nucleosomes or other shelterin complexes.

(B) Shelterin can recognize telomeric repeats via 3D search and does not require extensive 1D diffusion along DNA. For nanomolar concentrations of shelterin complexes and the association rate in Figure 7A, it takes only a few seconds until a free telomere repeat is bound and protected based on 3D search.

(C) Shelterin complexes do not detectably bind to each other, arguing against a telomeric architecture that is stabilized by shelterin filaments. Because shelterin functions as an independent DNA-binding unit (top), the number of telomere-bound shelterin complexes should be roughly proportional to telomere length (bottom), with approximately one shelterin per 100 bp. This prediction is in contrast with a cooperative model, in which shelterin complexes recruit each other, leading to a non-linear relationship (schematic gray dashed line). Our data do not exclude cooperativity induced by non-shelterin proteins or altered telomere topology.

et al., 2004). These experiments have indicated the presence of transiently ($k_{off} \approx 2$ min^{-1}) and stably ($k_{off} \approx 0.3$ min^{-1}) bound protein pools, with POT1 binding stably, TRF1 binding transiently, and TRF2 exhibiting both transient and stable binding to telomeres. The dissociation rate for transient binding is similar to the one we observed here for non-telomeric DNA, but the dissociation rate for stable binding is ten times larger than the one found here for telomeric DNA. This difference might be due to the competition by nucleosomes and other telomeric proteins in living cells, which we did not include in our experiments. However, differences might also arise from changes in shelterin stoichiometry caused by the overexpression of individual GFP-tagged shelterin subunits in living cells. It will be interesting to investigate these questions in the future.

Shelterin Assembly at Telomeres

Shelterin complexes can transiently bind to and diffuse along non-telomeric DNA. Similar behavior and similar effective diffusion coefficients were recently observed for TRF2 and, to some extent, for TRF1 (Lin et al., 2014), suggesting that shelterin interacts with non-telomeric DNA in a similar manner to its isolated dsDNA binding modules. Based on the ability of TRF1/2 to diffuse along DNA, Lin and colleagues proposed the attractive "tag-team proofreading" mechanism, in which individual

shelterin subunits bind independently to non-telomeric DNA and subsequently diffuse along the genome until they find their telomeric target site, where they meet each other and assemble the full shelterin complex (Lin et al., 2014). We find here that intact shelterin complexes (containing at least TRF2, Rap1, TIN2, TPP1, and POT1a) can stably exist in solution. Furthermore, we show that diffusion of shelterin complexes along DNA is considerably hindered by obstacles, including nucleosomes or other shelterin complexes, and that shelterin can readily recognize telomeric repeats by 3D search. The inability of shelterin to diffuse past either individual nucleosomes or other shelterin complexes suggests that 1D diffusion may play a limited role in the association of shelterin with telomeric repeats. Rather, cells might contain pre-formed shelterin complexes that can efficiently locate telomeres by a 3D diffusive search (Figure 7B). Such a search mechanism should also work efficiently in the context of chromatin, which exhibits a high density of nucleosomes and is decorated with a plethora of DNA-binding and chromatin-associated proteins (Déjardin and Kingston, 2009; Lejnine et al., 1995; Makarov et al., 1993). Indeed, most shelterin complexes in our experiments bound rapidly to telomeric repeats without diffusing across long stretches of flanking DNA beforehand. However, our data do not exclude that shelterin complexes diffuse over small distances (below our resolution limit) before binding to their target site, or that cells might contain a mixture of fully and partially assembled shelterin complexes that employ different strategies for telomere assembly.

Dynamic yet Persistent Telomere Protection Mechanism

Telomeres are not static entities; instead, they are subject to fluctuations in both length and protein content during the course of normal cellular growth and metabolism (Baird, 2008; O'Sullivan and Karlseder, 2010). Although telomeres must continuously be protected from cellular DNA damage sensors (Denchi and de Lange, 2007; Palm and de Lange, 2008; Sfeir and de Lange, 2012), they have to be replicated and elongated, which requires access of the responsible machinery to the telomeric DNA. Therefore, shelterin components might at least transiently be displaced from their telomeric binding sites. Furthermore, telomere elongation and replication generate new telomeric repeats, which have to be packaged and protected. Because telomere deprotection rapidly induces a DNA damage response that causes the appearance of γH2A.X foci on the timescale of several minutes (Konishi and de Lange, 2008), unprotected telomeric repeats must quickly be rebound by shelterin to maintain genome integrity.

We wondered whether the 3D assembly mechanism described above would function fast enough to bind a free telomeric repeat on the relevant timescale. To this end, we estimated the waiting time that is required until any newly created telomeric site in the cell nucleus would become bound by shelterin (Figure 7B). This waiting time is determined by the association rate of $\sim 6 \times 10^6$ $M^{-1}s^{-1}$ reported above and the cellular concentration of free shelterin complexes (Supplemental Experimental Procedures), which we estimated to be ~7 nM based on the concentration of free nucleoplasmic POT1 in HeLa cells (Takai et al., 2010). Using these values, the time a free telomeric repeat has to wait until it is bound by shelterin amounts to ~10 s. Although the precise concentration of free shelterin complexes and the association rate of unlabeled shelterin in the nucleus are not known, these estimates suggest that the 3D assembly mechanism above is fast enough to maintain a shelterin density that is sufficient to ensure persistent protection of telomeres from DNA damage sensors.

The Role of Shelterin in Higher-Order Structures of Telomeres

Telomeres have been proposed to have a compacted structure that might be mediated by strong shelterin-shelterin interactions (Bandaria et al., 2016). We observed long-lived interactions neither among shelterin complexes bound to the same DNA molecule, nor among shelterin complexes bound to different DNA molecules, and EM analysis did not reveal higher-order structures of the telomeric DNA. Although we cannot exclude the presence of transient shelterin-shelterin interactions that are not resolved in our assays, these findings suggest that each shelterin complex binds independently to its target site. Consequently, telomere compaction might require a special topology of shelterin-bound telomeric DNA that we did not mimic in our assays or might involve other cellular factors. Collectively, our data point to a shelterin configuration on telomeric DNA that resembles a "beads-on-a-string" pattern with large numbers of shelterin bound independently without making strong contacts with each other or with other parts of telomeric chromatin (Figure 7C). This model predicts that the amount of shelterin that is bound to a telomere is directly proportional to the number of telomeric repeats with one shelterin per ~100 bp, which means that the shelterin-mediated readout of telomere length is linear and does not involve a threshold telomere length below which the shelterin density would abruptly decline.

Conclusion

We have presented a strategy for purifying the mammalian shelterin complex and have studied its properties using a set of complementary techniques. We anticipate that the availability of reconstituted shelterin in conjunction with the assays developed here will improve our understanding of the biochemical and regulatory features of telomeres.

EXPERIMENTAL PROCEDURES

Protein Expression

Protein expression constructs were co-transfected into HEK293T cells using the standard calcium phosphate transfection protocol. After 8 hr, the medium was exchanged, and cells were harvested after 30 hr. To this end, cells were trypsinized, resuspended in media with serum, and washed two times in cold PBS, and the cell pellet was snap-frozen in liquid nitrogen and stored at −80°C. Protein complexes were purified as described in Supplemental Experimental Procedures.

Electrophoretic Mobility Shift Assays

For EMSAs, the indicated protein complexes and molarities were incubated with 0.2 nM DNA substrate in EMSA buffer (50 mM HEPES-KOH [pH 8.0], 50 mM LiCl, 0.1 mM DTT, 50 ng/μL β-Casein) (Chong et al., 1995) for 10 min on ice. Subsequently, samples were loaded on a 0.7% agarose gel and run in 1 × TAE buffer for 45 min at 100 V. The gel was fixed, washed in ddH_2O, dried, exposed overnight to a phosphorimager screen (GE Healthcare), and

scanned with Storm (Molecular Dynamics). For EMSA supershifts, protein and DNA were incubated for 5 min on ice before the antibody was added. After a further incubation time of 5 min on ice, the samples were loaded onto an agarose gel and processed as described above.

DNA Curtains

DNA curtains were assembled on nanofabricated slides as described previously (Greene et al., 2010). Measurements were carried out at room temperature. The running buffer contained 40–70 mM Tris-HCl (pH 7.8) and 0.2–1.0 mg/mL BSA. For experiments at high ionic strength, proteins were injected in 50 mM HEPES (pH 7.6), 300 mM KGlut, and 0.2 mg/mL BSA. Curtains were visualized using TIRF microscopy (Supplemental Experimental Procedures).

Electron Microscopy Direct Mounting Method

Aliquots of the samples containing DNA-protein complexes were mixed with a buffer containing spermidine and adsorbed onto copper grids coated with a thin carbon film glow-charged shortly before sample application. After adsorption of the samples for 2–3 min, the grids were washed with EM grade water and dehydrated through a graded ethanol series from 25% to 95%. Following quick air drying, the grids were subjected to rotary shadow casting with tungsten at 2×10^{-6} torr. Samples were examined in an FEI T12 TEM equipped with a Gatan 2k × 2k SC200 charged-couple device (CCD) camera at 40 kV. Adobe Photoshop software was used to arrange images into panels for publication (Griffith and Christiansen, 1978).

Statistical Methods

Errors for EMSAs (Figure 2) were obtained by calculating the SD of multiple replicates. Errors for histograms of binding positions (Figures 3E, 4A, 4B, and S4B), survival plots (Figures 4B, 4F, 4I, and S4A), and association rate measurements (Figures 4J, 4K, S6C, and S6D) were determined based on bootstrapping with replacement (Efron and Tibshirani, 1993).

SUPPLEMENTAL INFORMATION

Supplemental Information includes Supplemental Experimental Procedures, seven figures, one table, and three movies and can be found with this article online at http://dx.doi.org/10.1016/j.celrep.2016.12.005.

AUTHOR CONTRIBUTIONS

F.E. designed and conducted all the DNA curtain experiments (Figures 3, 4, 5, 6, S2A, and S3–S7). K.K. purified and characterized the shelterin complexes and did the Southern blots (Figures 1, 2, S1, and S2B). S.W. conducted the electron microscopy experiments (Figures 6E and 6F). F.E., K.K., J.D.G., E.C.G., and T.d.L. designed experiments, evaluated data, and wrote the manuscript.

ACKNOWLEDGMENTS

We thank the Proteomics Resource Center at The Rockefeller University for help with the mass spectrometry analysis. F.E. was supported by an EMBO long-term fellowship (EMBO ALTF 187-2014). K.K. was supported by an EMBO long-term fellowship (EMBO ALTF-1044-2011) and funds from the Women & Science Fellowship Program at The Rockefeller University. J.D.G. was supported by grants from the NIH (GM31819 and ES13373). E.C.G. was supported by a grant from the NIH (R35GM118026). T.d.L. was supported by a grant from the NIH (5R01AG016642). T.d.L. is an ACS Research Professor.

Received: September 7, 2016
Revised: November 13, 2016
Accepted: November 30, 2016
Published: January 3, 2017

REFERENCES

Baird, D.M. (2008). Telomere dynamics in human cells. Biochimie *90*, 116–121.

Bandaria, J.N., Qin, P., Berk, V., Chu, S., and Yildiz, A. (2016). Shelterin protects chromosome ends by compacting telomeric chromatin. Cell *164*, 735–746.

Baumann, P., and Cech, T.R. (2001). Pot1, the putative telomere end-binding protein in fission yeast and humans. Science *292*, 1171–1175.

Benarroch-Popivker, D., Pisano, S., Mendez-Bermudez, A., Lototska, L., Kaur, P., Bauwens, S., Djerbi, N., Latrick, C.M., Fraisier, V., Pei, B., et al. (2016). TRF2-mediated control of telomere DNA topology as a Mechanism for chromosome-end protection. Mol. Cell *61*, 274–286.

Bianchi, A., Smith, S., Chong, L., Elias, P., and de Lange, T. (1997). TRF1 is a dimer and bends telomeric DNA. EMBO J. *16*, 1785–1794.

Bianchi, A., Stansel, R.M., Fairall, L., Griffith, J.D., Rhodes, D., and de Lange, T. (1999). TRF1 binds a bipartite telomeric site with extreme spatial flexibility. EMBO J. *18*, 5735–5744.

Broccoli, D., Smogorzewska, A., Chong, L., and de Lange, T. (1997). Human telomeres contain two distinct Myb-related proteins, TRF1 and TRF2. Nat. Genet. *17*, 231–235.

Celli, G.B., and de Lange, T. (2005). DNA processing is not required for ATM-mediated telomere damage response after TRF2 deletion. Nat. Cell Biol. *7*, 712–718.

Choi, K.H., Farrell, A.S., Lakamp, A.S., and Ouellette, M.M. (2011). Characterization of the DNA binding specificity of Shelterin complexes. Nucleic Acids Res. *39*, 9206–9223.

Chong, L., van Steensel, B., Broccoli, D., Erdjument-Bromage, H., Hanish, J., Tempst, P., and de Lange, T. (1995). A human telomeric protein. Science *270*, 1663–1667.

Court, R., Chapman, L., Fairall, L., and Rhodes, D. (2005). How the human telomeric proteins TRF1 and TRF2 recognize telomeric DNA: A view from high-resolution crystal structures (vol 6, pg 39, 2005). EMBO Rep. *6*, 191–191.

de Lange, T. (2005). Shelterin: The protein complex that shapes and safeguards human telomeres. Genes Dev. *19*, 2100–2110.

Déjardin, J., and Kingston, R.E. (2009). Purification of proteins associated with specific genomic Loci. Cell *136*, 175–186.

Denchi, E.L., and de Lange, T. (2007). Protection of telomeres through independent control of ATM and ATR by TRF2 and POT1. Nature *448*, 1068–1071.

Doksani, Y., Wu, J.Y., de Lange, T., and Zhuang, X. (2013). Super-resolution fluorescence imaging of telomeres reveals TRF2-dependent T-loop formation. Cell *155*, 345–356.

Efron, B., and Tibshirani, R.J. (1993). An Introduction to the Bootstrap (Chapman & Hall).

Gaullier, G., Miron, S., Pisano, S., Buisson, R., Le Bihan, Y.V., Tellier-Lebègue, C., Messaoud, W., Roblin, P., Guimarães, B.G., Thai, R., et al. (2016). A higher-order entity formed by the flexible assembly of RAP1 with TRF2. Nucleic Acids Res. *44*, 1962–1976.

Greene, E.C., Wind, S., Fazio, T., Gorman, J., and Visnapuu, M.L. (2010). DNA curtains for high-throughput single-molecule optical imaging. Methods Enzymol. *472*, 293–315.

Griffith, J.D., and Christiansen, G. (1978). Electron microscope visualization of chromatin and other DNA-protein complexes. Annu. Rev. Biophys. Bioeng. *7*, 19–35.

Griffith, J.D., Comeau, L., Rosenfield, S., Stansel, R.M., Bianchi, A., Moss, H., and de Lange, T. (1999). Mammalian telomeres end in a large duplex loop. Cell *97*, 503–514.

Hanaoka, S., Nagadoi, A., and Nishimura, Y. (2005). Comparison between TRF2 and TRF1 of their telomeric DNA-bound structures and DNA-binding activities. Protein Sci. *14*, 119–130.

Hockemeyer, D., Daniels, J.P., Takai, H., and de Lange, T. (2006). Recent expansion of the telomeric complex in rodents: Two distinct POT1 proteins protect mouse telomeres. Cell *126*, 63–77.

Hockemeyer, D., Palm, W., Else, T., Daniels, J.P., Takai, K.K., Ye, J.Z., Keegan, C.E., de Lange, T., and Hammer, G.D. (2007). Telomere protection by

mammalian Pot1 requires interaction with Tpp1. Nat. Struct. Mol. Biol. *14*, 754–761.

Karlseder, J., Broccoli, D., Dai, Y., Hardy, S., and de Lange, T. (1999). p53- and ATM-dependent apoptosis induced by telomeres lacking TRF2. Science *283*, 1321–1325.

Karlseder, J., Hoke, K., Mirzoeva, O.K., Bakkenist, C., Kastan, M.B., Petrini, J.H.J., and de Lange, T. (2004). The telomeric protein TRF2 binds the ATM kinase and can inhibit the ATM-dependent DNA damage response. PLoS Biol. *2*, E240.

Kaur, P., Wu, D., Lin, J., Countryman, P., Bradford, K.C., Erie, D.A., Riehn, R., Opresko, P.L., and Wang, H. (2016). Enhanced electrostatic force microscopy reveals higher-order DNA looping mediated by the telomeric protein TRF2. Sci. Rep. *6*, 20513.

Kibe, T., Osawa, G.A., Keegan, C.E., and de Lange, T. (2010). Telomere protection by TPP1 is mediated by POT1a and POT1b. Mol. Cell. Biol. *30*, 1059–1066.

Konishi, A., and de Lange, T. (2008). Cell cycle control of telomere protection and NHEJ revealed by a ts mutation in the DNA-binding domain of TRF2. Genes Dev. *22*, 1221–1230.

Lei, M., Podell, E.R., and Cech, T.R. (2004). Structure of human POT1 bound to telomeric single-stranded DNA provides a model for chromosome end-protection. Nat. Struct. Mol. Biol. *11*, 1223–1229.

Lejnine, S., Makarov, V.L., and Langmore, J.P. (1995). Conserved nucleoprotein structure at the ends of vertebrate and invertebrate chromosomes. Proc. Natl. Acad. Sci. USA *92*, 2393–2397.

Lin, J., Countryman, P., Buncher, N., Kaur, P., e, L., Zhang, Y., Gibson, G., You, C., Watkins, S.C., Piehler, J., et al. (2014). TRF1 and TRF2 use different mechanisms to find telomeric DNA but share a novel mechanism to search for protein partners at telomeres. Nucleic Acids Res. *42*, 2493–2504.

Liu, D., Safari, A., O'Connor, M.S., Chan, D.W., Laegeler, A., Qin, J., and Songyang, Z. (2004). PTOP interacts with POT1 and regulates its localization to telomeres. Nat. Cell Biol. *6*, 673–680.

Loayza, D., and De Lange, T. (2003). POT1 as a terminal transducer of TRF1 telomere length control. Nature *423*, 1013–1018.

Loayza, D., Parsons, H., Donigian, J., Hoke, K., and de Lange, T. (2004). DNA binding features of human POT1: A nonamer 5′-TAGGGTTAG-3′ minimal binding site, sequence specificity, and internal binding to multimeric sites. J. Biol. Chem. *279*, 13241–13248.

Makarov, V.L., Lejnine, S., Bedoyan, J., and Langmore, J.P. (1993). Nucleosomal organization of telomere-specific chromatin in rat. Cell *73*, 775–787.

Martínez, P., Thanasoula, M., Muñoz, P., Liao, C., Tejera, A., McNees, C., Flores, J.M., Fernández-Capetillo, O., Tarsounas, M., and Blasco, M.A. (2009). Increased telomere fragility and fusions resulting from TRF1 deficiency lead to degenerative pathologies and increased cancer in mice. Genes Dev. *23*, 2060–2075.

Mattern, K.A., Swiggers, S.J., Nigg, A.L., Löwenberg, B., Houtsmuller, A.B., and Zijlmans, J.M. (2004). Dynamics of protein binding to telomeres in living cells: Implications for telomere structure and function. Mol. Cell. Biol. *24*, 5587–5594.

Nandakumar, J., and Cech, T.R. (2012). DNA-induced dimerization of the single-stranded DNA binding telomeric protein Pot1 from Schizosaccharomyces pombe. Nucleic Acids Res. *40*, 235–244.

O'Sullivan, R.J., and Karlseder, J. (2010). Telomeres: Protecting chromosomes against genome instability. Nat. Rev. Mol. Cell Biol. *11*, 171–181.

Palm, W., and de Lange, T. (2008). How shelterin protects mammalian telomeres. Annu. Rev. Genet. *42*, 301–334.

Palm, W., Hockemeyer, D., Kibe, T., and de Lange, T. (2009). Functional dissection of human and mouse POT1 proteins. Mol. Cell. Biol. *29*, 471–482.

Sfeir, A., and de Lange, T. (2012). Removal of shelterin reveals the telomere end-protection problem. Science *336*, 593–597.

Sfeir, A., Kosiyatrakul, S.T., Hockemeyer, D., MacRae, S.L., Karlseder, J., Schildkraut, C.L., and de Lange, T. (2009). Mammalian telomeres resemble fragile sites and require TRF1 for efficient replication. Cell *138*, 90–103.

Stansel, R.M., de Lange, T., and Griffith, J.D. (2001). T-loop assembly in vitro involves binding of TRF2 near the 3′ telomeric overhang. EMBO J. *20*, 5532–5540.

Takai, K.K., Hooper, S., Blackwood, S., Gandhi, R., and de Lange, T. (2010). In vivo stoichiometry of shelterin components. J. Biol. Chem. *285*, 1457–1467.

Takai, K.K., Kibe, T., Donigian, J.R., Frescas, D., and de Lange, T. (2011). Telomere protection by TPP1/POT1 requires tethering to TIN2. Mol. Cell *44*, 647–659.

Taylor, D.J., Podell, E.R., Taatjes, D.J., and Cech, T.R. (2011). Multiple POT1-TPP1 proteins coat and compact long telomeric single-stranded DNA. J. Mol. Biol. *410*, 10–17.

van Steensel, B., and de Lange, T. (1997). Control of telomere length by the human telomeric protein TRF1. Nature *385*, 740–743.

van Steensel, B., Smogorzewska, A., and de Lange, T. (1998). TRF2 protects human telomeres from end-to-end fusions. Cell *92*, 401–413.

Wang, F., Podell, E.R., Zaug, A.J., Yang, Y., Baciu, P., Cech, T.R., and Lei, M. (2007). The POT1-TPP1 telomere complex is a telomerase processivity factor. Nature *445*, 506–510.

Wu, L., Multani, A.S., He, H., Cosme-Blanco, W., Deng, Y., Deng, J.M., Bachilo, O., Pathak, S., Tahara, H., Bailey, S.M., et al. (2006). Pot1 deficiency initiates DNA damage checkpoint activation and aberrant homologous recombination at telomeres. Cell *126*, 49–62.

Wu, P., Takai, H., and de Lange, T. (2012). Telomeric 3′ overhangs derive from resection by Exo1 and Apollo and fill-in by POT1b-associated CST. Cell *150*, 39–52.

Xin, H., Liu, D., Wan, M., Safari, A., Kim, H., Sun, W., O'Connor, M.S., and Songyang, Z. (2007). TPP1 is a homologue of ciliate TEBP-beta and interacts with POT1 to recruit telomerase. Nature *445*, 559–562.

Ye, J.Z., Hockemeyer, D., Krutchinsky, A.N., Loayza, D., Hooper, S.M., Chait, B.T., and de Lange, T. (2004). POT1-interacting protein PIP1: A telomere length regulator that recruits POT1 to the TIN2/TRF1 complex. Genes Dev. *18*, 1649–1654.

Zhu, X.D., Küster, B., Mann, M., Petrini, J.H., and de Lange, T. (2000). Cell-cycle-regulated association of RAD50/MRE11/NBS1 with TRF2 and human telomeres. Nat. Genet. *25*, 347–352.